

# Statistical analysis of the electromechanical behavior of AgMg sheathed $\text{Bi}_2\text{Sr}_2\text{CaCu}_2\text{O}_{8+x}$ superconducting tapes using Weibull distributions

A. L. Mbaruku<sup>a)</sup>

National High Magnetic Field Laboratory, Tallahassee, Florida 32310

J. Schwartz

National High Magnetic Field Laboratory, Tallahassee, Florida 32310

and Department of Mechanical Engineering, FAMU-FSU College of Engineering, Tallahassee, Florida 32310

(Received 6 November 2006; accepted 29 January 2007; published online 13 April 2007)

Manufacturing of AgMg sheathed  $\text{Bi}_2\text{Sr}_2\text{CaCu}_2\text{O}_{8+x}$  superconducting tapes involves multiple processes. Microstructural studies across tape sections have shown that the microstructure is nonuniform across the tape. These nonuniformities are largely due to manufacturing defects, even in well-controlled manufacturing processes. Consequently, the electrical and mechanical properties vary in these different sections. Here, we report results from analyzing the electromechanical properties of AgMg sheathed  $\text{Bi}_2\text{Sr}_2\text{CaCu}_2\text{O}_{8+x}$  tapes in different sections using a statistical approach. 24 samples were studied at strains of 0%, 0.25%, and 0.349% for a total of 72 samples. The probability of electrical and mechanical failures of the tapes is then analyzed using two- and three-parameter Weibull distributions. It is found that the mechanical failure of these tapes is homogeneous, consistent with failure in the AgMg sheath, but that the electromechanical failure is inhomogeneous within the conductor and as a function of strain, indicating that this failure is dictated by failure in the inhomogeneous ceramic oxide superconducting filaments. This has important implications for the designs of superconducting magnets. © 2007 American Institute of Physics. [DOI: 10.1063/1.2715844]

## I. INTRODUCTION

High temperature superconducting (HTS) tapes are promising conductors for many applications, including high field superconducting magnets generating magnetic fields greater than 20 T. This potential was demonstrated in an insert superconducting magnet developed jointly by the National High Magnetic Field Laboratory (NHMFL) and Oxford Superconducting Technology (OST) as an effort toward developing a 25 T superconducting magnet.<sup>1</sup> The superconducting insert magnet produced 5.11 T in a 19.94 T background field generated by a resistive magnet.<sup>2</sup> The insert magnet was constructed using AgMg-sheathed  $\text{Bi}_2\text{Sr}_2\text{CaCu}_2\text{O}_{8+x}$  (Bi2212) tapes. This insert coil used several kilometers of Bi2212/AgMg multifilamentary tapes fabricated by the powder-in-tube (PIT) method, which is currently regarded as the standard method for large-scale manufacture of such tapes.

When fabricating the AgMg Bi2212 composite tapes, the goal is to obtain high critical current density ( $J_c$ ) and engineering current density ( $J_E$ ). This is a complex process, however, that involves interactions between many factors, including the characteristics of starting precursor powder, deformation process, final shape and size, heat treatment schedule, oxygen content and uniformity, structural unifor-

mity of the ceramic filaments, etc.<sup>3</sup> It is not uncommon for  $J_c$  to vary by 10%–20% from sample to sample within a batch of Bi2212 tape.

Relationships between the critical current ( $I_c$ ) and mechanical strain ( $\epsilon$ ) of Bi2212 have been reported previously by a number of authors.<sup>4–6</sup> Since the earliest work,<sup>7,8</sup> data have been reported in terms of a critical strain value  $\epsilon_c$ . In this model,  $I_c$  is nearly constant and quasireversible for  $\epsilon < \epsilon_c$  and then decreases sharply and rapidly for  $\epsilon > \epsilon_c$ . In this model, which is an accurate description for the behavior of individual wires and tapes, the failure is associated with the brittle failure of individual Bi2212 filaments. Furthermore, previously we reported the effects of processing defects on stress-strain- $I_c$  for such tapes.<sup>9</sup> It was shown that the tapes have varying microstructure along the length. Consequently, the mechanical and superconducting properties varied from one section to another. As a result, while the traditional critical strain model is useful to describe the behavior of an individual sample, it does not capture the behavior of a batch of conductor. As magnets are built of long lengths of conductor, understanding this collective behavior is essential. Thus, it is important to make a correlated, statistical analysis on the mechanical and electrical properties of Bi2212 conductors.

One well known statistical analysis approach is the Weibull distribution which has been used to characterize mechanical properties of both metals and ceramics.<sup>10,11</sup> There are two primary forms of Weibull cumulative distribution functions (cdf's): two- and three-parameter distributions, and

<sup>a)</sup>Electronic mail: mbaruku@magnet.fsu.edu

depending on the data, one can use either.<sup>12,13</sup> The three-parameter Weibull distribution function is given by

$$F(x; \alpha, \beta, \gamma) = 1 - e^{-[(x - \gamma)/\alpha]^\beta}, \quad \alpha \geq 0, \\ \beta \geq 0, \quad \gamma \geq 0, \quad (1)$$

where  $x$  is variable and  $\alpha$ ,  $\beta$ , and  $\gamma$  are the scale, shape, and location parameters, respectively. In the two-parameter form, the location parameter  $\gamma$  is zero.

In this work, we use both two- and three-parameter Weibull distributions to investigate the probability of failure of Bi2212 tapes mechanically and electrically. When considering the yield stress, the left side of Eq. (1) represents the probability that the yield stress for the AgMg sheathed Bi2212 tape is less than or equal to  $x$ . If we consider the critical current as the variable, then the left side of Eq. (1) represents the probability that the critical current of the AgMg sheathed Bi2212 tape at a given strain condition is less than or equal to  $x$ .

The parameters of  $F(x; \alpha, \beta, \gamma)$  are estimated from the experimental data using a linear regression. This method involves transforming Eq. (1) into Eq. (2),

$$1 - F(x; \alpha, \beta, \gamma) = e^{-[(x - \gamma)/\alpha]^\beta}. \quad (2)$$

Taking double logarithms on both sides of Eq. (2) and rearranging,

$$\ln \left\{ \ln \left[ \frac{1}{1 - F(x; \alpha, \beta, \gamma)} \right] \right\} = \beta \ln(x - \gamma) - \beta \ln(\alpha). \quad (3)$$

The function  $F(x; \alpha, \beta, \gamma)$  is determined from the experimental data using the median rank of  $x$  after arranging the data in increasing order of magnitude. That is, let  $x_{(i)}$  be the experimental data set. Then,  $i=1$  corresponds to the minimum  $x_{(i)}$  and  $i=n$  corresponds to the maximum  $x_{(i)}$ . The median rank is given by

$$F(x_{(i)}; \alpha, \beta, \gamma) = \frac{i - 0.3}{(n + 0.4)}. \quad (4)$$

By applying linear regression to paired values of  $\ln(x_{(i)} - \gamma)$ , and the left side of Eq. (3), the parameters  $\alpha$ ,  $\beta$ , and  $\gamma$  are obtained.  $\gamma$  is usually unknown when the regression is performed. MICROSOFT EXCEL solver was used to maximize the linearity of the paired data by subtracting  $\gamma$  from each  $x$  and constraining  $\beta < 6$ , which is a limit for a two-parameter Weibull distribution ( $\gamma=0$ ). The method is described in more detail in Ref. 12.

Three strain conditions are used in this work:  $\varepsilon=0\%$ ,  $\varepsilon=0.25\%$ , and  $0.349\%$ . Weibull parameters are estimated as detailed above and the respective distributions for mechanical and electrical behaviors are plotted for each strain condition.

## II. EXPERIMENTAL WORK

### A. Samples

All samples for this work were derived from one batch of superconductor supplied by OST. The batch average  $I_c$  (4.2 K, self-field) from 24 samples is 379.88 A with a stan-

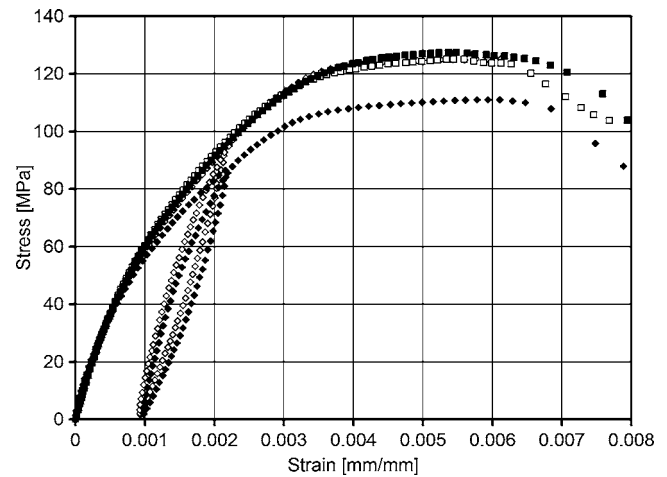


FIG. 1. Room-temperature stress-strain curves for AgMg sheathed  $\text{Bi}_2\text{Sr}_2\text{CaCu}_2\text{O}_x$  tape. Young's modulus is 70 GPa, yield stress is  $\sim 126.7$  MPa (based on 0.2% offset) and yield strain ( $\varepsilon_y$ ) of 0.349%.

ard deviation of 87.82 A. Average dimensions of the tapes are 5.00 mm wide, 0.21 mm thick, and 45 mm in length. More details on the conductor can be found in Ref. 14.

## B. Experiments

Stress-strain testing was first performed to measure yield stress  $\sigma_y$ , ultimate strength  $\sigma_{\text{ult}}$ , and Young's modulus of the conductor. These tests also were important for determining the strain at which yielding occurred ( $\varepsilon_y$ ). Samples tested at  $\varepsilon=0\%$  were cut to size and  $I_c$  measurements were performed without straining. Samples strained to  $\varepsilon=0.25\%$  and  $\varepsilon=0.349\%$  were uniaxially strained prior to  $I_c$  measurements. Mechanical straining of the samples was performed at room temperature using a linear tensile testing device that was previously described in detail.<sup>9,15</sup> The system includes force and displacement transducers, and LabVIEW is used to control the stepper motor, data acquisition from transducers via digital multimeters and their conversion into stress and strain. Additional details are found in Ref. 16.  $I_c$  was measured at 4.2 K, self-field, using a four-point method with a  $1 \mu\text{V}/\text{cm}$  electric field criterion. To make a statistical analysis of the conductor failure, a total of 24 replication tests were performed for each strain condition.

## III. RESULTS

### A. Mechanical properties

Stress-strain graphs resulting from the tensile tests are shown in Fig. 1. Note that the curves do not have well defined straight lines in either the initial loading or the unloading and reloading portions that were performed at approximately 0.2% strains. The Young moduli were obtained by connecting the end points of the loop formed during the unloading and reloading portions of the curves. The average of the Young modulus is 70 GPa, the yield stress based on a 0.2% offset criterion is 126.7 MPa, and the ultimate strength is 132.5 MPa. The yield strain is 0.349%.

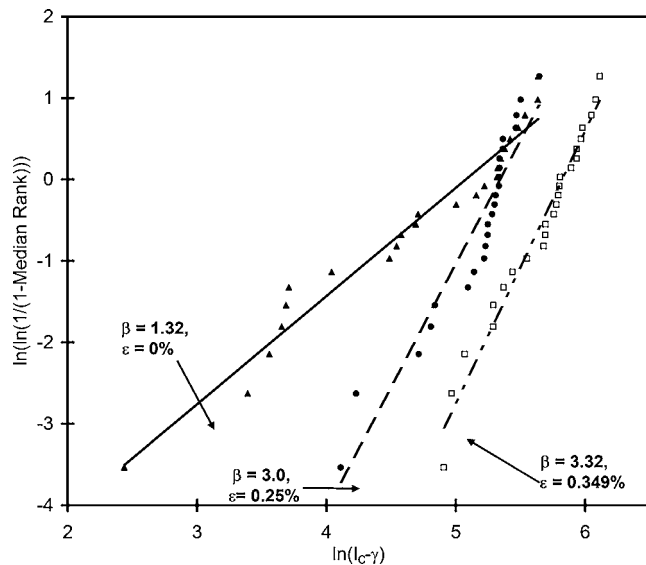


FIG. 2. The regression lines obtained during calculation of the Weibull parameters from  $I_c$  data with  $\varepsilon=0\%$ ,  $0.25\%$ , and  $0.349\%$ .  $\beta$  represents the slope of the regression lines for each strain value,  $\gamma$  is the offset value subtracted from each data to maximize the linear relationship of the regression line, and  $\alpha$  is a measure of distribution of the data in the Weibull distribution.

## B. Electrical failure

The regression results from the critical current data for  $\varepsilon=0\%$ ,  $0.25\%$ , and  $0.349\%$  are shown in Fig. 2 and the resulting Weibull distributions for the current are shown in Fig. 3. Table I shows the corresponding  $\alpha$ ,  $\beta$ , and  $\gamma$  for these data as a function of applied strain. As the applied strain is increased,  $\alpha$  and  $\beta$  increased with increasing strain, while  $\gamma$  decreased with increasing strain.

The results of the replication tests at the yield strain ( $\varepsilon_y=0.349\%$ ) are presented in Table II. The resulting regression line for the yield stresses is shown in Fig. 4. From the yield stress data, the values of  $\beta=1.84$ ,  $\alpha=18.0$ , and  $\gamma=109.84$  are obtained.

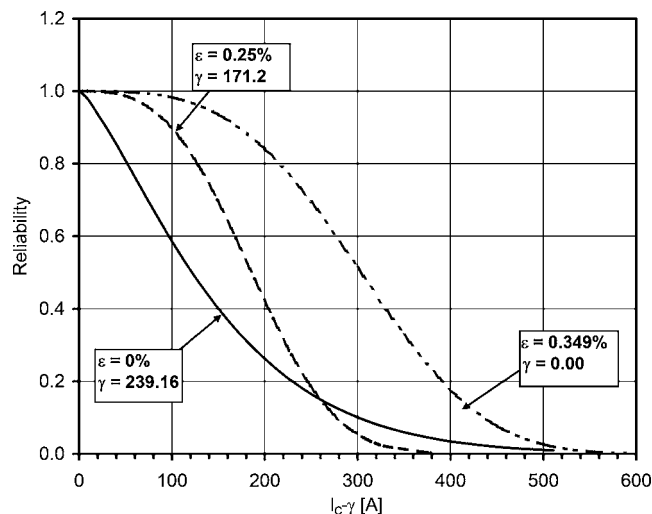


FIG. 3. The Weibull distributions obtained from  $I_c$  data with  $\varepsilon=0\%$ ,  $0.25\%$ , and  $0.349\%$ . The location parameters  $\gamma$  are the current values below which there is 100% reliability. These values decrease with increasing strain, as expected, and becomes zero at the yield strain.

TABLE I.  $\alpha$ ,  $\beta$ , and  $\gamma$  values from  $I_c$  data as a function of applied uniaxial strain applied to the samples prior to  $I_c$  measurements.

Applied strain (%)	Beta ( $\beta$ )	Alpha ( $\alpha$ )	Gamma ( $\gamma$ )
0.0	1.32	160.42	239.16
0.25	3.00	209.85	171.20
0.349	3.32	338.30	0.0

Using the obtained values of shape, scale, and location parameters, the Weibull probability distribution for yield stress is plotted in Fig. 5. This curve represents the distribution of samples that have not yielded by the 0.2% offset method after straining to the batch average  $\varepsilon_y$ .

## IV. DISCUSSION

The tensile test results in Fig. 1 show that the samples tested have only small variations in their mechanical properties up about 45 MPa. There are differences, however, just above this point, with some samples being weaker than others. On the other hand, as seen in Table II, there are significant variations on the stress value at the yield point from all samples that were used in the replication tests. These variations are most likely caused by the differences in the microstructures of the different sections of the tape. Note that the yield stresses shown in Table II are for individual samples determined by their respective values of Young's modulus.

The slopes of the lines in Fig. 2 determine the  $\beta$  values which determine the failure rates of the critical current at the different strain values. In general,  $\beta < 1$  indicates a high initial failure rate that decays as the  $I_c$  increases. That is, the reliability decreases sharply at low values of  $I_c$ , and then slowly thereafter. If  $\beta = 1$ , the failure rate is constant for all  $I_c$ . For  $\beta > 1$  the reliability decreases slowly at first and then relatively sharply above some value of  $I_c$ . As  $\beta$  increases further, the Weibull distribution becomes less gradual and the decrease in reliability becomes rapid. The  $\alpha$  values measure the data distribution. That is, how the  $I_c$  is spread in the cumulative probability function. For a fixed value of  $\beta$ , increasing  $\alpha$  spreads the distribution to the right and reduces the probability peak. The location parameter  $\gamma$  is an offset value for given set of data and is the value below which there is no failure.

Thus, considering Fig. 5, no samples have a yield stress lower than 109.84 MPa (the  $\gamma$  value for this dataset), and yield stress values can be (albeit very rarely) as high as 150 MPa. 80% of the samples have a yield stress below 133 MPa. The low value of  $\beta=1.84$  is consistent with the rapid decrease in reliability (increase in failure rate) as the stress increases above  $\gamma$ . For a metal-ceramic composite of this nature, this distribution is expected.

It is interesting, however, to consider the three Weibull distribution curves in Fig. 3 and the corresponding  $\alpha$ ,  $\beta$ , and  $\gamma$  values in Table I. Note that in Fig. 3, what is plotted is reliability versus  $(I_c - \gamma)$ ; thus all three curves begin at (1,0), indicating that none have a critical current lower than the value of  $\gamma$  that corresponds to the level of strain (this is the definition of  $\gamma$ ). For currents greater than  $\gamma$ , however, the reliability curve decreases most rapidly for  $\varepsilon=0$  and less

TABLE II. Results for replication tests on the AgMg sheathed  $\text{Bi}_2\text{Sr}_2\text{CaCu}_2\text{O}_x$  tapes. The yield stress values are obtained by the 0.2% offset method and correspond to 0.349% strain. All critical current values were obtained at 4.2 K, self-field using the four-point method with a  $1 \mu\text{V}/\text{cm}$  electric field criterion.

Sample No.	Yield stress (MPa)	Critical current (A)	Sample No.	Yield stress (MPa)	Critical current (A)
1	136.04	277.97	13	133.20	415.01
2	146.71	338.49	14	135.10	244.30
3	129.93	445.20	15	137.25	382.70
4	121.46	288.30	16	117.92	387.12
5	121.10	130.96	17	131.95	278.84
6	129.39	485.00	18	127.10	369.74
7	120.72	443.46	19	129.92	319.53
8	106.40	229.09	20	122.83	298.94
9	109.94	414.20	21	106.60	295.18
10	118.69	193.69	22	137.30	275.85
11	134.15	323.92	23	122.20	239.60
12	125.34	381.35	24	131.44	221.20

rapidly with increasing strain. This is consistent with the increasing values of  $\alpha$ . The curves are also consistent with the values of  $\beta$  for the three strain conditions. That is, failure occurs first for data with lowest value of  $\beta$ . Thus, it appears that one effect of mechanical strain is to increase the inhomogeneity of electrical failure within a length of conductor.

Figure 6 replots the data of Fig. 3, but instead shows reliability versus  $I_c$ . Thus, in this case, each strain value shows a reliability that is identically 1 until the corresponding  $\gamma$  value is reached. Here, one sees that for  $\varepsilon = \varepsilon_y$ , the reliability decreases for all values of  $I_c > 0$ . For  $\varepsilon = 0$ ,  $\gamma = 239$  A, which is only 63% of the average  $I_c$  of the conductor, indicating the scatter in conductor performance (in this case, it is not a mechanical or cool down effect that is being observed since all samples have experienced the same processing conditions). The data for  $\varepsilon = 0.25\%$ , which is about 70% of the yield strain, have  $\gamma = 171$  A, which is 45% of the zero-strain batch average. At this strain value, the reliability for  $I_c = 380$  A (the batch average) is only 38%. This is significant because, if one applies the traditional model<sup>4,6</sup> where

$I_c$  changes by 2%–3% with increasing strain to  $\varepsilon_y$ , one would expect  $I_c(\varepsilon = 0.25) \sim 0.97I_c(\varepsilon = 0)$ . Even if one considers a current value that is one standard deviation lower than the batch average  $I_c$  ( $I = 379.88 - 87.82 \text{ A} = 292.06 \text{ A}$ ), the reliability for  $\varepsilon = 0.25\%$  is about 84%; i.e., at  $\varepsilon = 0.25$ , 16% of the conductor has  $I_c$  more than one standard deviation below the batch average.

These results have significant and direct impact on the design of magnets using long lengths of conductor. If the traditional model is used, significant strain margin must be incorporated into the design to allow for statistical variations in electromechanical properties. Some strain margin is obtained by operating currents well below  $I_c$ . This margin is, in fact, essential, and magnets that attempt to push to both the current and strain limits are going to fail due to the distribution of electromechanical properties within a batch of conductor.

It is important to note that these results are based on a batch of Bi2212 tape that was state-of-the-art circa 2003, but

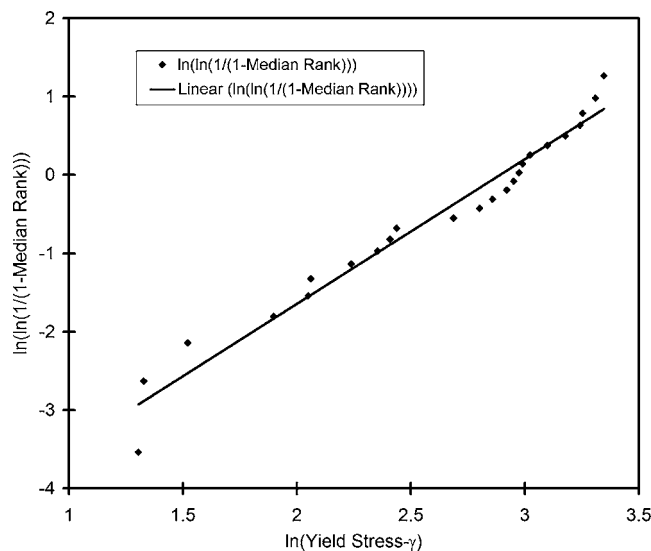


FIG. 4. The regression line obtained when estimating Weibull parameters from yield stress data for AgMg sheathed  $\text{Bi}_2\text{Sr}_2\text{CaCu}_2\text{O}_x$  tape.

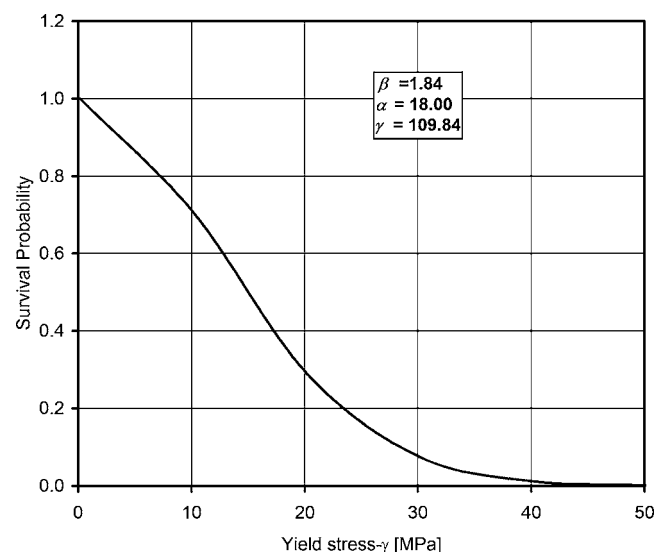


FIG. 5. Weibull reliability distribution for stress for the AgMg sheathed  $\text{Bi}_2\text{Sr}_2\text{CaCu}_2\text{O}_x$  tape. The distribution shows the fraction of samples that have not yet yielded as defined by the 0.2% yield stress.

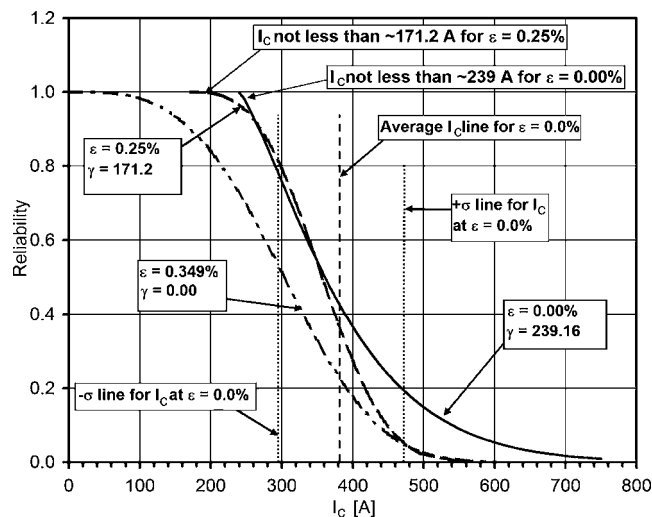


FIG. 6. The data from Fig. 3 are replotted here by shifting each curve to the right by its corresponding  $\gamma$  value. Thus, these are plots of reliability vs  $I_c$  for  $\epsilon=0\%$ ,  $0.25\%$ , and  $0.349\%$ .

that significant improvements in Bi2212 conductor technology, and, in particular, in the development of high current density round wires, have been obtained in the ensuing three years. It will be particularly interesting to determine if the variability in electromechanical properties decreases if the conductor homogeneity (as defined by critical current variations) increases. Ultimately, however, whichever behavior is more variable must be the primary consideration in applications of these materials to superconducting magnets.

Furthermore, one might expect this work to analyze the data using fiber bundle models rather than a Weibull model because the conductors are multifilamentary. After heat treatment, however, the Bi2212 conductors have significant bridging of filaments through the Ag matrix, so although their original construct is multifilamentary, their final form behaves as an electrical monofilament.<sup>17,18</sup> Thus, a fiber bundle model that considers the load distribution upon breakage of individual filaments is not appropriate.<sup>19</sup> Rather, the Weibull statistics used here is suitable since the current flow is a weakest-link phenomena.

## V. CONCLUSIONS

Statistical analysis of Bi2212 conductors using Weibull distributions has been used on  $I_c$  and yield stress data obtained from samples strained to 0%, 0.25%, and 0.349%. All samples were derived from the same batch of AgMg sheathed Bi2212 tape made by the powder-in-tube method. Variations in the electromechanical properties have been observed from the experimental data obtained from these samples. This is believed to be largely contributed to by the

microstructural differences along the different sections of the tape. It was found that although the stress-strain behavior and mechanical failure of the conductor are fairly uniform from sample to sample, indicating homogeneous mechanical properties, the electromechanical failure (critical current dependence on strain) shows significant variations from sample to sample and as a function of strain. Thus, it appears that the mechanical properties of the conductor are dictated by the AgMg sheath and are thus homogeneous, but the electromechanical behavior is governed by failure in the less-homogeneous and flaw-driven ceramic oxide filaments that carry the transport current in the superconducting state. These results have significant implications for the designs of magnets utilizing ceramic oxide superconductors.

## ACKNOWLEDGMENTS

This work was supported by the Office of Naval Research through the Center of Advanced Power Systems and the National Science Foundation through the National High Magnetic Field Laboratory. The authors would like to thank Oxford Superconducting Technology, and, in particular, Dr. Ken Marken and Dr. Hanping Miao, for providing the AgMg sheathed Bi2212 tape that was used in this work.

- <sup>1</sup>H. W. Weijers *et al.*, IEEE Trans. Appl. Supercond. **2**, 1396 (2003).
- <sup>2</sup>H. W. Weijers, U. P. Trociewitz, K. Marken, M. Meinesz, H. Miao, and J. Schwartz, Supercond. Sci. Technol. **17**, 636 (2004).
- <sup>3</sup>K. R. Marken, H. Miao, J. M. Sowa, J. A. Parrell, and S. Hong, IEEE Trans. Appl. Supercond. **1**, 3252 (2001).
- <sup>4</sup>B. ten Haken and H. J. ten Kate, IEEE Trans. Appl. Supercond. **2**, 1298 (1995).
- <sup>5</sup>R. Wesche, A. M. Fuchs, B. Jakob, and G. Pasztor, Cryogenics **36**, 419 (1996).
- <sup>6</sup>B. ten Haken, A. Godeke, H. Schuver, and H. J. ten Kate, IEEE Trans. Magn. **4**, 2720 (1996).
- <sup>7</sup>B. ten Haken, A. Beuink, and H. J. ten Kate, IEEE Trans. Appl. Supercond. **2**, 2034 (1997).
- <sup>8</sup>J. Schwartz, H. Sekine, T. Asano, T. Kuroda, K. Inoue, and H. Maeda, IEEE Trans. Magn. **27**, 1247 (1991).
- <sup>9</sup>A. L. Mbaruku, K. R. Marken, M. Meinesz, H. Miao, P. V. P. S. S. Sastry, and J. Schwartz, IEEE Trans. Appl. Supercond. **2**, 3522 (2003).
- <sup>10</sup>J. Y. Pastor, J. LLorca, P. Poza, I. de Francisco, R. I. Merino, and J. I. Peña, J. Eur. Ceram. Soc. **25**, 1225 (2005).
- <sup>11</sup>J. C. Fernandes, P. M. Amaral, L. G. Rosa, and N. Shohoji, Ceram. Int. **26**, 203 (2000).
- <sup>12</sup>A. J. Hallinan, J. Quality Technol. **25**, 85 (1993).
- <sup>13</sup>J. I. McCool, J. Quality Technol. **30**, 119 (1998).
- <sup>14</sup>K. R. Marken, H. Miao, M. Meinesz, B. Czabaj, and S. Hong, IEEE Trans. Appl. Supercond. **13**, 3335 (2003).
- <sup>15</sup>A. L. Mbaruku, I. Rutel, U. P. Trociewitz, H. W. Weijers, and J. Schwartz, Adv. Cryog. Eng. **50**, 700 (2004).
- <sup>16</sup>J. Schwartz, B. C. Amm, H. Garmestani, D. K. Hilton, and Y. Hascicek, IEEE Trans. Appl. Supercond. **7**, 2038 (1997).
- <sup>17</sup>H. Miao, K. R. Marken, M. Meinesz, B. Czabaj, and S. Hong, IEEE Trans. Appl. Supercond. **15**, 2554 (2005).
- <sup>18</sup>T. G. Holesinger, J. A. Kennison, K. R. Marken, H. Miao, M. Meinesz, and S. Campbell, IEEE Trans. Appl. Supercond. **15**, 2562 (2005).
- <sup>19</sup>F. Kun, S. Zapperi, and H. J. Herrmann, Eur. Phys. J. B **17**, 269 (2000).